

# Subcellular localization of the *Hpa* RxLR effector repertoire identifies a tonoplast-associated protein HaRxL17 that confers enhanced plant susceptibility

Marie-Cécile Caillaud<sup>1</sup>, Sophie J. M. Piquerez<sup>1</sup>, Georgina Fabro<sup>1,†</sup>, Jens Steinbrenner<sup>2</sup>, Naveed Ishaque<sup>1</sup>, Jim Beynon<sup>2</sup> and Jonathan D. G. Jones<sup>1,\*</sup>

<sup>1</sup>The Sainsbury Laboratory, John Innes Centre, Norwich Research Park, Norwich NR4 7UH, UK, and

<sup>2</sup>School of Life Sciences, Wellesbourne Campus, The University of Warwick, Wellesbourne, Warwick CV35 9EF, UK

Received 30 June 2011; revised 6 September 2011; accepted 8 September 2011; published online 29 November 2011.

\*For correspondence (e-mail jonathan.jones@tsl.ac.uk).

<sup>†</sup>Present address: CIQUIBIC-CONICET, Departamento de Química Biológica, Facultad de Ciencias Químicas, Universidad Nacional de Córdoba, Córdoba X500HUA, Argentina.

## SUMMARY

Filamentous phytopathogens form sophisticated intracellular feeding structures called haustoria in plant cells. Pathogen effectors are likely to play a role in the establishment and maintenance of haustoria in addition to their better-characterized role in suppressing plant defence. However, the specific mechanisms by which these effectors promote virulence remain unclear. To address this question, we examined changes in subcellular architecture using live-cell imaging during the compatible interaction between the oomycete *Hyaloperonospora arabidopsidis* (*Hpa*) and its host *Arabidopsis*. We monitored host-cell restructuring of subcellular compartments within plant mesophyll cells during haustoria ontogenesis. Live-cell imaging highlighted rearrangements in plant cell membranes upon infection, in particular to the tonoplast, which was located close to the extra-haustorial membrane surrounding the haustorium. We also investigated the subcellular localization patterns of *Hpa* RxLR effector candidates (HaRxLs) *in planta*. We identified two major classes of HaRxL effector based on localization: nuclear-localized effectors and membrane-localized effectors. Further, we identified a single effector, HaRxL17, that associated with the tonoplast in uninfected cells and with membranes around haustoria, probably the extra-haustorial membrane, in infected cells. Functional analysis of selected effector candidates *in planta* revealed that HaRxL17 enhances plant susceptibility. The roles of subcellular changes and effector localization, with specific reference to the potential role of HaRxL17 in plant cell membrane trafficking, are discussed with respect to *Hpa* virulence.

**Keywords:** oomycete, effector, RxLR, haustoria, nucleus, membrane.

## INTRODUCTION

Eukaryotic filamentous pathogens such as rust and powdery mildew fungi, and oomycetes including the downy mildew *Hyaloperonospora arabidopsidis* (*Hpa*) and *Phytophthora* species, form specialized feeding structures in their host cells that are called haustoria. Haustoria-producing pathogens include some of the most destructive plant parasites, causing huge economic losses in important agricultural industries and damage to natural ecosystems (Haverkort *et al.*, 2008; Singh *et al.*, 2011). Despite this, little is known about the molecular basis of pathogenicity in this important class of phytopathogens, mainly due to the fact that most of these organisms are difficult to culture and thus are not suitable for molecular genetic approaches.

Haustroria are sophisticated but poorly understood structures. They are topologically distinct from the host-cell cytoplasm, and surrounded by an extra-haustorial membrane (EHM) of unknown origin. It has been shown that numerous host plasma membrane (PM) proteins are absent from the EHM of powdery mildew-infected *Arabidopsis*, suggesting that the EHM may originate from *de novo* membrane assembly or from the PM through a mechanism for excluding host proteins (Koh *et al.*, 2005). Using *in vivo* live-cell imaging, the *Arabidopsis* syntaxin PEN1, which is involved in protein trafficking and disease resistance at the plant cell wall, has been localized to powdery mildew haustorial encasements (Meyer *et al.*, 2009), whereas the

broad-spectrum mildew resistance protein RPW8.2 from *Arabidopsis* has been reported to be localized to the EHM (Wang *et al.*, 2009). During the formation and maturation of haustoria, callose and other plant cell-wall material is often deposited to form a collar around the haustorial neck, which can subsequently expand to encase the entire haustorium (Bushnell, 1972; Meyer *et al.*, 2009). In contrast to subcellular dynamics at pathogen penetration sites (Howard and Valent, 1996; Takemoto *et al.*, 2003, 2006; Genre *et al.*, 2005), the rearrangement of plant cell compartments in cells hosting oomycete haustoria remains uncharacterized.

In many plant–pathogen interactions, pathogen-encoded effectors are key pathogenicity determinants that modulate plant innate immunity and enable parasitic infection (Kamoun, 2007; Hogenhout *et al.*, 2009). Effectors may play a role during the transition of the infection site into a metabolic sink, in addition to their classically defined role in suppressing plant defences (Ellis *et al.*, 2009; Hok *et al.*, 2010; Voegelé and Mendgen, 2011). Recently, a number of effectors conferring avirulence has been identified from haustoria-forming pathogens (Birch *et al.*, 2006; Win *et al.*, 2007; De Wit *et al.*, 2009; Valent and Khang, 2010; Bailey *et al.*, 2011). Rust and oomycete avirulent proteins are usually expressed in haustoria, and hypersensitive response (HR) usually initiates after haustoria are formed. This correlation suggests that haustoria play a critical role in delivering effector proteins into the infected host cell (Ellis *et al.*, 2009; Hok *et al.*, 2010). This hypothesis is supported by immunolocalization studies of secreted proteins from rust pathogens (Kemen *et al.*, 2005, 2011; Rafiqi *et al.*, 2010).

In contrast to fungal effectors, for which no conserved region has been yet identified, oomycete effectors usually contain a secretory signal peptide and a conserved domain featuring the motif RxLR, followed by a motif with a high frequency of acidic (D/E) residues, and a C-terminal domain(s) associated with virulence function (Rehmany *et al.*, 2005; Birch *et al.*, 2006; Win *et al.*, 2007). To date, nine avirulent oomycete RxLR effectors have been identified, including ATR1 and ATR13 from *Hpa* (Allen *et al.*, 2004; Rehmany *et al.*, 2005). These intracellular effectors are presumed to be first secreted by the oomycetes (Whisson *et al.*, 2007; Gilroy *et al.*, 2011), and are then taken up by the host cell by an unknown mechanism involving the N-terminal RxLR motif (Kale *et al.*, 2010). The sequencing of several oomycete genomes, including *Hpa* (Baxter *et al.*, 2010), has allowed prediction of a large number of effector genes that share N-terminal sequences with the known effectors (Win *et al.*, 2007; Baxter *et al.*, 2010). The *Hpa* genome contains 134 high-confidence effector gene candidates (HaRxL genes), including the known effector genes ATR1 and ATR13, significantly fewer than *Phytophthora* genomes (Tyler *et al.*, 2006; Jiang *et al.*, 2008).

To assess the function of RxLR effector candidates in plant immunity, screening methods have recently been developed (Cabral *et al.*, 2011; Fabro *et al.*, 2011). Use of these methods has shown that the majority of the HaRxLs (approximately 70%) positively contributed to bacterial virulence, and this was positively correlated with their ability to suppress plant-triggered immunity (Cabral *et al.*, 2011; Fabro *et al.*, 2011). However, the mechanisms by which *Hpa* effectors promote virulence are still largely unknown.

The localization of pathogen effectors inside the plant cell gives an indication of their mode of action (Downe *et al.*, 2009; Schornack *et al.*, 2010). Increasing evidence suggests that host protein secretion is an important process that mediates plant resistance against pathogens, and that pathogen virulence factors may target intracellular trafficking to suppress host immunity (Huckelhoven, 2007; Kalde *et al.*, 2007; Robatzek, 2007; Nomura *et al.*, 2011; Wu *et al.*, 2011). In addition, bacterial effectors have been shown to localize to the nucleus of the plant cell where they may modulate plant gene expression (Gurlebeck *et al.*, 2006; Poueymiro and Genin, 2009). In contrast with bacteria and necrotrophic fungi, many obligate biotroph pathogens are recalcitrant to stable transformation. In addition, when transformants are generated, translocation of the effector in the host cell cannot usually be observed as the fluorescent signal is diluted in the plant cell cytoplasm (Whisson *et al.*, 2007; Boevink *et al.*, 2011). To circumvent this problem, fluorescent-tagged effector protein can be expressed directly in the plant cell (Kelley *et al.*, 2010; Rafiqi *et al.*, 2010; Schornack *et al.*, 2010). Using this approach, the RxLR effector Avr3a was localized *in planta* during infection using *Agrobacterium tumefaciens* delivery of tagged effectors (Bos *et al.*, 2010; Boevink *et al.*, 2011). Thus, use of cell biology techniques to assess the virulence function of oomycete effectors is an emerging field. Further, Bozkurt *et al.* (2011) report focal recruitment of *P. infestans* Avr-blb2:GFP fusions to haustorial membranes during the *P. infestans*/*Nicotiana benthamiana* interaction.

In order to study the molecular dialogue between *Hpa* and *Arabidopsis*, we developed an *in vivo* cell biology approach to analyse changes to subcellular compartments within the host cell and identify the compartments targeted by *Hpa* effectors. By transiently expressing 49 *Hpa* RxLR effector candidates (HaRxLs) fused to fluorescent tags *in planta*, we defined major classes of HaRxLs that accumulate in the plant cell nucleus and plant membranes. *In planta* functional analysis revealed that the membrane-localized effector HaRxL17 enhances plant susceptibility. This study allowed us to identify a role for plant cell membrane trafficking in modulation of *Hpa* virulence.

## RESULTS

### Dynamics of host plant cell compartments during *Hpa* infection, highlighting the close association between the plant cell nucleus and *Hpa* haustoria

We used a collection of Col-0 Arabidopsis fluorescent protein-tagged lines to unveil the organization of plant cell compartments *in vivo* in mesophyll cells hosting haustoria (Table 1). Ten-day-old seedlings of Arabidopsis marker lines were inoculated with virulent *Hpa* Noco2 isolate. Infected mesophyll tissues were then observed at an early stage of infection [4 days after infection (DAI)] by live-cell imaging. At this stage, young developing haustoria were observed near the growing tip of *Hpa* hyphae, and mature haustoria encased in callose-rich depositions were observed along the ageing hyphae.

We observed aggregation of ER membranes and accumulation of Golgi bodies around young *Hpa* haustoria, suggesting that production and secretion of plant materials are activated around the haustoria ( $n > 20$ ; Figure 1a and Figure S1a) as previously described by Chou (1970). *In vivo* Z-stack confocal imaging showed that actin microfilaments formed large bundles in cytoplasmic strands focused around the haustorium (asterisk) and the adjacent nucleus (arrow) ( $n = 9$ , Figure 1b). Using free GFP as a nuclear/cytoplasmic marker, we confirmed the presence of cytoplasm around the haustorium ( $n > 50$ , Figure 1c). Notably, we observed that the nucleus was always associated with developing haustoria in mesophyll cells ( $n > 50$ , Figure 1b,c). This association between haustoria and nuclei in mesophyll cells was confirmed using the plant nuclear marker line H2A-GFP ( $n = 15$ , Figure S1b). We observed that mitochondria accumulated around haustoria ( $n = 15$ , Figure S1e), whereas chloroplasts and peroxisomes appeared to be free in the cytoplasm of mesophyll cells hosting haustoria ( $n = 15$ , Figure S1d). This observation was surprising as the peroxisome-associated marker PEN2 localized around the haustorium during *Hpa* infection ( $n = 5$ , Figure S1e).

### Plasma membrane markers are excluded from the EHM, but the tonoplast is located close to the membrane surrounding the haustorium

It has been shown that numerous host PM proteins are absent from the EHM of fungi-infected Arabidopsis, suggesting that the EHM originates from *de novo* assembly of plant membranes or remodelling of the existing PM with exclusion of host proteins. Therefore, we investigated the subcellular localization of a PM marker in order to verify its exclusion from the EHM of oomycete-infected Arabidopsis. Ten-day-old Arabidopsis seedlings expressing the GFP-tagged aquaporin PIP1;4 were inoculated with the *Hpa* virulent isolates Noco2 and Waco9. Infected mesophyll tissues were then observed at an early stage of infection (4 DAI) by live-cell imaging. In non-infected cells (Figure 1d), GFP-tagged PIP1;4 localized to the rough ER and the PM, as previously reported (Geldner *et al.*, 2009). In *Hpa*-infected cells, no GFP-PIP1;4 signal was observed at the EHM. However, a weak signal was detected in the cytoplasm around haustoria corresponding to the ER ( $n = 15$ ; Figure 1d).

We next determined the localization of the PEN1-GFP and RPW8.2-YFP fusion proteins under the control of native promoter (Np) during *Hpa* infection. In non-infected cells, PEN1-GFP localizes to the PM in mesophyll cells (Collins *et al.*, 2003), but RPW8.2-YFP is not detectable (Wang *et al.*, 2007). At an early stage of infection (3 DAI), PEN1-GFP is associated with the callose ring present at the neck of the developing haustorium ( $n > 20$ , Figure S2a), but RPW8.2-YFP is localized to vesicle-like bodies surrounding haustoria ( $n = 10$ , Figure S2b). No signal at the EHM was observed for either marker at early stages of haustorium formation. Later during infection, PEN1-GFP and RPW8.2-YFP localized to haustorium encasements ( $n > 20$ , Figure S2c,d), as described for powdery mildew haustoria. Taken together, these results confirm the exclusion of PM markers from the EHM of *Hpa* haustoria and their accumulation in the callose-rich haustorium encasements as previously reported for fungal pathogens.

**Table 1** Summary of plant cell compartment rearrangements upon infection with *Hpa* in Arabidopsis mesophyll cells

Subcellular compartment	Location in <i>Hpa</i> -infected mesophyll cells	Marker lines used	Reference
Endoplasmic reticulum	Surrounding haustoria	ER-GK	Nelson <i>et al.</i> (2007)
Golgi	Accumulating around haustoria	g-GK	Nelson <i>et al.</i> (2007)
Actin cytoskeleton	Surrounding haustoria	GFP-ABD-GFP	Pang <i>et al.</i> (1998)
Cytoplasm	Surrounding haustoria	Free GFP	This study
Nucleus	Moving close to the haustoria	H2A-GFP	Unpublished data from Peter Shaw's laboratory, John Innes Centre, Norwich, UK
Mitochondria	Accumulating around haustoria	mt-GK	Nelson <i>et al.</i> (2007)
Peroxisome	Staying free in the cytoplasm	px-CK	Nelson <i>et al.</i> (2007)
Chloroplast	Staying free in the cytoplasm	Autofluorescence	This study
Plasma membrane	Remaining excluded from the EHM	PIP1;4-RFP	Geldner <i>et al.</i> (2009)
Tonoplast	Strongly labelling membrane around haustoria	$\gamma$ -TIP-GFP	Nelson <i>et al.</i> (2007)



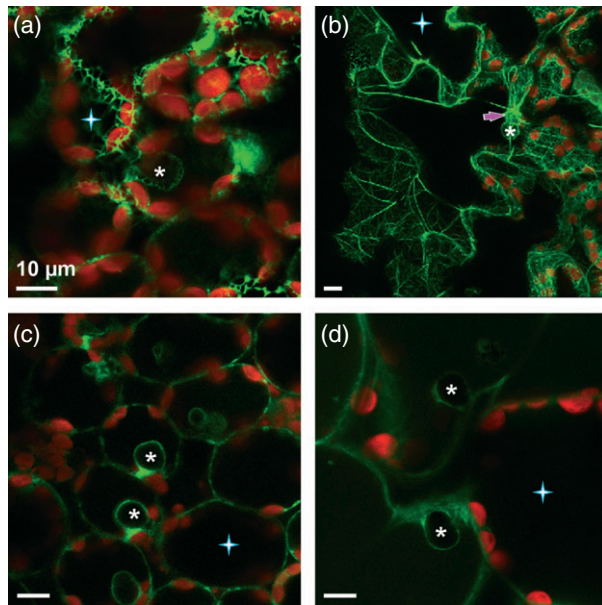


**Figure 1.** *In vivo* rearrangements of plant cell compartments in mesophyll cells hosting *Hpa* haustoria.

Live-cell imaging of fluorescent protein-tagged cell components in Arabidopsis mesophyll cells hosting *Hpa* haustoria 4 days after infection (4 DAI). The green colour corresponds to the GFP signal; red corresponds to chloroplast autofluorescence. Asterisks indicate the position of the haustorium, blue stars indicate an uninfected cell, and pink arrows indicate nuclei. Scale bars = 10 µm.

(a) Single-plane confocal imaging of the ER-GK line (ER marker) 4 DAI with *Hpa*.

(b) Z-stack confocal imaging of the GFP-ABD-GFP line (actin marker) 4 DAI with *Hpa*.

(c) Single-plane confocal imaging of free GFP in Arabidopsis, 4 DAI with *Hpa*.

(d) Single-plane confocal imaging of the PIP1;4-RFP line (PM marker), 4 DAI with *Hpa*.

Previous ultrastructure studies of plant cells hosting haustoria described close proximity between the EHM and the tonoplast, resulting in a very thin layer of host-cell cytoplasm (approximately 0.1 µm between the EHM and the tonoplast) (Chou, 1970; Mims *et al.*, 2004). Using *in vivo* confocal imaging, we detailed the behaviour of the tonoplast over a time course of *Hpa* infection. We showed that, in contrast to the exclusion of PM markers around haustoria, the tonoplast intrinsic protein  $\gamma$ -TIP-GFP strongly labelled the vicinity of the EHM in young haustoria ( $n > 25$ ; Figure 2a). At this stage of infection (4 DAI), the central vacuole of mesophyll cells hosting haustoria resembled the vacuole in a non-infected mesophyll cell ( $n > 25$ ; Figure 2a), as previously reported by Chou (1970). Later during infection (7 DAI), very bright  $\gamma$ -TIP-GFP membrane labelling was observed in the lumen space of the vacuole around mature haustoria ( $n > 25$ ; Figure 2b,c). The highly fluorescent structures observed (including lines, arcs and circles) are very similar to the double tonoplast cytoplasmic invaginations into vacuoles described in leaves and cotyledons of Arabid-

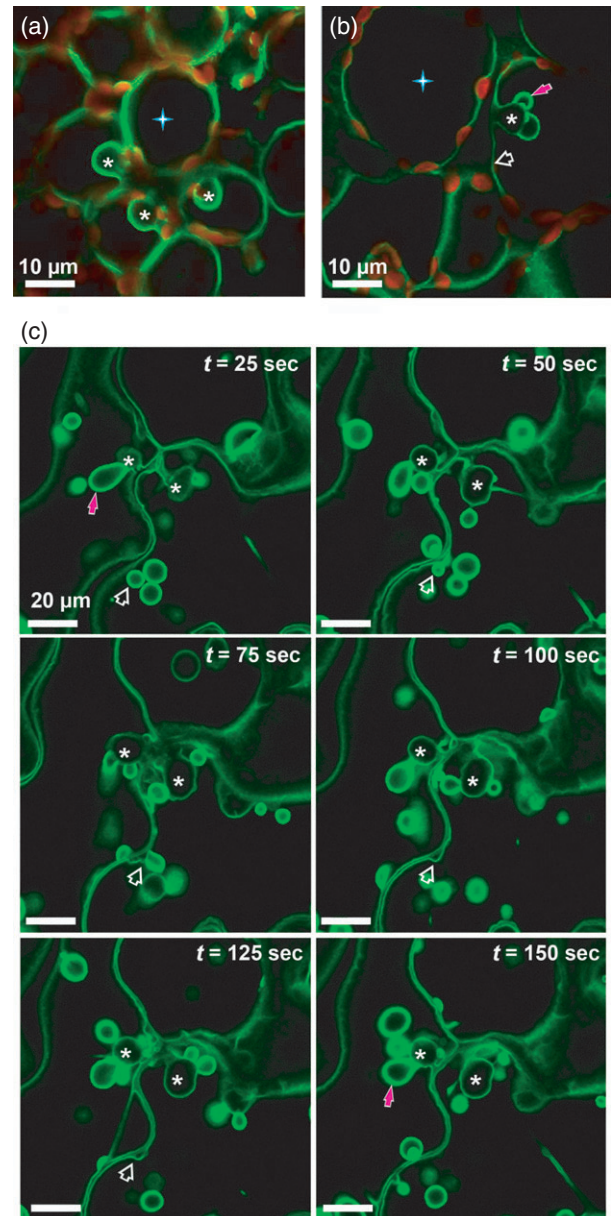


**Figure 2.** *In vivo* dynamics of the vacuolar trafficking in mesophyll cells hosting *Hpa* haustoria.

The green colour corresponds to the fluorescent signal in the  $\gamma$ -TIP-GFP line; red corresponds to chloroplast autofluorescence. Asterisks indicate the position of the haustorium in the cell, blue stars indicate non-infected cells, and solid and open arrows indicate bulbs. Scale bars = 10 µm.

(a) Single-plane confocal imaging of the  $\gamma$ -TIP-GFP line 4 DAI with *Hpa*.

(b) Single-plane confocal imaging of the  $\gamma$ -TIP-GFP line 6 DAI with *Hpa*.

(c) *In vivo* time-lapse imaging of  $\gamma$ -TIP-GFP-labelled tonoplast 6 DAI.

opsis (Saito *et al.*, 2002), and are termed 'bulbs'. Such bulbs were rarely observed in surrounding non-infected cells ( $n > 25$ ; Figure 2b). *In vivo* time-lapse imaging of  $\gamma$ -TIP-GFP-labelled tonoplast membrane revealed highly dynamic vacuole trafficking around mature haustoria in infected mesophyll cells. Bulbs accumulated around mature

haustoria, but appeared to be unable to fuse with membranes surrounding haustoria ( $n = 7$ ; Figure 2b,c and Video Clips S1 and S2). Within the same infected cell, other bulbs trafficked freely, budding from and fusing to the tonoplast of the central vacuole.

### Subcellular localization of the *Hpa* effector repertoire reveals that the host nucleus and membrane network are the main targeted compartments

As some plant compartments are highly dynamic upon *Hpa* infection, we investigated which host-cell compartments are targeted by the effectors of this obligate biotroph to promote its virulence. To address this question, we designed a fluorescence imaging-based screen *in planta* to assess the subcellular localization of a collection of *Hpa* RxLR effector candidates (HaRxLs) from the *Hpa* reference isolate Emoy2 (Fabro *et al.*, 2011; Table S1). We used a recently developed transient assay (Downen *et al.*, 2009; Schornack *et al.*, 2010) to express oomycete and fungal effectors *in planta*. We generated fluorescent protein-tagged versions of 49 HaRxLs downstream of their signal peptide cleavage site. Chimeric constructs were expressed transiently in *Nicotiana benthamiana* using *A. tumefaciens* infiltration (Table S1), and were imaged 24–48 h post-infiltration. The stability of the fusion protein was verified by Western blot analysis for each candidate (Figure S3).

Of the 49 HaRxLs tested, 16 (33%) localized to the plant cell nucleus and the cytoplasm, including the avirulent ATR1<sup>Emoy2</sup> allele (Figure 3a,b, Figure S5 and Table S1). We identified three HaRxLs that strictly localized to the plant cell cytoplasm (Figure 3c, Figure S4 and Table S1) and one localized to the vacuole (Figure 3d). The majority (66%, merging the strictly nuclear-localized and the nuclear-cytoplasmic) of HaRxLs targeted the plant cell nucleus (Figure 3a,e–j, Figure S4, Figure S5 and Table S1), but *in silico* analysis showed that only 37.5% of the 16 HaRxLs that strictly localized to the nucleus carried a canonical nuclear localization signal (Table S1). Of the 16 HaRxLs that localized to the plant cell nucleus, we identified specific sub-nuclear localizations: GFP-HaRxL18 was excluded from the nucleolus ( $n = 15$ , Figure 3e); RFP-HaRxLL108 localized to the nucleoplasm and possibly labelled weakly the nucleolus ( $n = 20$ , Figure 3f); GFP-HaRxLL3b showed strong labelling of the nucleolus and fiber-like structures in the nucleoplasm ( $n = 10$ , Figure 3g); GFP-HaRxL36 showed strong nucleoplasmic labelling and nucleolar cap-like structures ( $n = 10$ , Figure 3h); GFP-ATR13<sup>Emoy2</sup> concentrated into the cell nucleolus ( $n = 25$ , Figure 3i) and GFP-HaRxLL470b showed strong labelling of the nucleolus and speckles in the nucleoplasm ( $n = 15$ , Figure 3j). Of the 16 HaRxLs that localized to the plant cell nucleus, we found that 11 were nucleolar localized, including the virulent allele ATR13<sup>Emoy2</sup>.

In addition to the nuclear-localized HaRxLs, we identified a second class of effectors that targeted the plant membrane

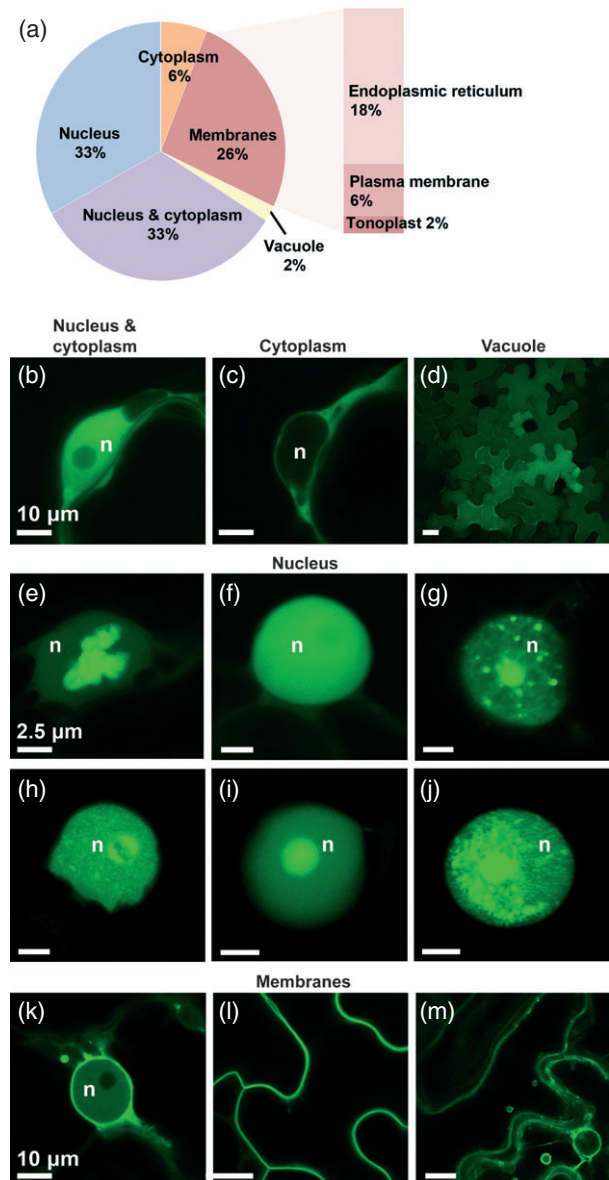


**Figure 3.** HaRxLs predominantly localize to the plant cell nucleus and the membrane trafficking network.

(a) *In planta* HaRxL localization in each cell compartment. (b–m) Representative images showing the diversity of subcellular localization of fluorescent protein-tagged HaRxLs when transiently expressed in *N. benthamiana*. n, nucleus. Scale bars = 10  $\mu$ m (b–d, k–m) and 2.5  $\mu$ m (e–j).

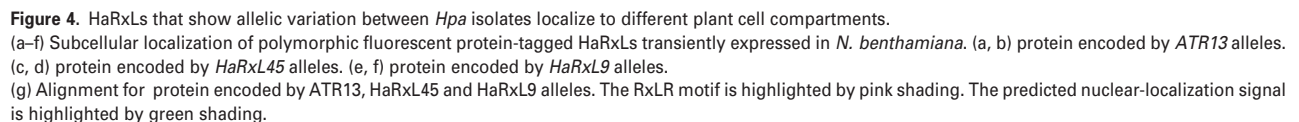
trafficking network. Thirteen HaRxLs (26%) localized to various plant membranes. Of these, nine localized to the ER network, including HaRxLL495b (Figure 3k, Figure S4 and Table S1). Surprisingly, only three candidates, including HaRxL77, localized to the plant PM (Figure 3l and Figure S4). The PM-localized proteins HaRxL77 and HaRxL146 are both predicted to be potentially post-translationally modified by *N*-myristoylation, whereas HaRxL47 is predicted to have two



In order to validate the screening system in *N. benthamiana*, we next generated stable *Arabidopsis* transgenic lines expressing single GFP-tagged HaRxLs. We randomly selected 20 candidates that localized to different plant cell compartments (Table S1). For all of the GFP-tagged HaRxLs tested, we observed the same subcellular localization in both systems, thus validating the survey. Only 20% of the localizations observed were correctly predicted *in silico*.

For some HaRXLs, evidence of polymorphism between eight *Hpa* isolates (Cala2, Emco5, Emoy2, Hiks1, Hind2, Maks9,

Noco2 and Waco9) has been found (Fabro *et al.*, 2011). We used transient assays in *N. benthamiana* to assess the subcellular localization of three HaRxLs that show allelic variation between *Hpa* isolates, ATR13, HaRxL45 and HaRxL9. Live-cell imaging showed that YFP-ATR13<sup>Maks9</sup> and GFP-ATR13<sup>Emoy2</sup> localized to the plant cell nucleolus, whereas GFP-ATR13<sup>Emco5</sup> localized to the plant nucleus and cytoplasm ( $n > 30$ , Figures 3i and 4a,b). This difference in localization can be explained by the presence of a predicted nuclear localization signal in both ATR13<sup>Maks9</sup> and ATR13<sup>Emoy2</sup> that is absent in ATR13<sup>Emco5</sup> (Figure 4g). GFP-HaRxL45<sup>Emoy2</sup> localized to the plant nucleoplasm and nucleolus (Figure 4c), but GFP-HaRxL45<sup>Hiks1</sup> localized to the plant cytoplasm and the nucleus and was excluded from the nucleolus (Figure 4d). These differences in subcellular localizations were not correlated with polymorphism with regard to a predicted nuclear localization signal in the sequences of HaRxL45 alleles (Figure 4g). We also found that, while HaRxL9<sup>Emoy2</sup> was localized to the nucleus and cytoplasm (Figure 4e), HaRxL9<sup>Noco2</sup> localized to the plant PM (Figure 4f). Thus, for the tested polymorphic HaRxLs, amino acid polymorphisms cause a change in their subcellular localization *in planta*, which may influence their virulence functions.



### HaRxL17 and HaRxL77 effectors confer enhanced plant susceptibility

The role of membrane-localized HaRxLs during *Hpa* infection in Arabidopsis was assessed by examining their effect on pathogen virulence. We selected three candidates that localized to different membranes, ER-localized HaRxLL495b (Figure 3k), PM-localized HaRxL77 (Figure 3l) and tonoplast-localized HaRxL17 (Figure 3m). We first verified that these candidates were expressed *in planta* during *Hpa* infection using RT-PCR (Figure S6). We next generated Arabidopsis Col-0 plants that stably expressed a single GFP-tagged HaRxL. We confirmed the presence of fusion proteins in the tested transgenic plants by Western blot analysis (Figure S7). These lines, and the GFP-ATR13 line as a control, were challenged with the virulent *Hpa* Waco9 isolate.

Two independent GFP-ATR13-expressing transgenic lines were more susceptible to *Hpa* than Col-0 ( $P > 0.001$ ; Figure 5a), consistent with the observation that ATR13 positively contributes to pathogen virulence inside host cells (Sohn *et al.*, 2007). In contrast, the transgenic lines expressing HaRxLL495b did not show any difference in susceptibility to *Hpa* compared with Col-0 (Figure 5b). Independent transgenic lines expressing GFP-HaRxL17 and GFP-HaRxL77 were more susceptible to *Hpa* than wild-type plant ( $P > 0.001$ ; Figure 5c,d). Thus, the HaRxL17 and HaRxL77 effectors enhance plant susceptibility during a compatible interaction between *Hpa* and its host.

We next analysed whether HaRxL localization changed during infection with *Hpa* using live-cell imaging. We first confirmed that, in Arabidopsis transgenic lines, independently of the level of expression, GFP-tagged HaRxLs localized to the same plant cell compartment as observed in a transient assay in *N. benthamiana* ( $n > 30$ , Figure S8). Using a biochemical approach, we next confirmed that GFP-HaRxL17 accumulates in the microsomal fraction in Arabidopsis transgenic line (Figure S9). Subcellular localization of GFP-tagged HaRxLs at 3 DAI with *Hpa* showed that GFP-ATR13 localized to the plant cell nucleolus in *Hpa* Waco9 haustorium-invaded mesophyll cells ( $n = 20$ , Figure 5e). HaRxLL495b-GFP localized around the haustoria and in the plant cell nucleus ( $n = 10$ , Figure 5f). GFP-HaRxL77 still localized at the PM in the infected cells, but also at the haustorial neck ( $n = 20$ , Figure 5g). In addition, a weak fluorescent signal corresponding to GFP-HaRxL77 was observed around haustoria (Figure 5g). Thus, no re-localization of nucleolar-localized ATR13, PM-localized HaRxL77 or ER-localized HaRxLL495b was observed in *Hpa* Waco9 haustorium-invaded mesophyll cells. However, in transgenic lines expressing GFP-tagged HaRxL17, strong re-localization of this effector around the haustoria was observed in early stages of *Hpa* infection ( $n > 20$ , Figure 5h). At this stage, no signal in the tonoplast or PM was observed in infected cells ( $n > 20$ , Figure 5h). Thus, the *Hpa* effector

HaRxL17, which suppressed plant immunity during a compatible interaction between *Hpa* and its host, re-localized around haustoria at early stages of infection.

### HaRxL17 suppresses plant immunity during an incompatible interaction and localizes at the EHM

We tested whether any of the selected HaRxLs could compromise effector-triggered immunity. In Arabidopsis Col-0, *RPP4* confers resistance to the *Hpa* Emoy2 isolate (van der Biezen *et al.*, 2002). Transgenic lines stably expressing GFP-ATR13, HaRxLL495b-GFP, GFP-HaRxL77 or GFP-HaRxL17 were therefore challenged with *Hpa* Emoy2.

In wild-type Col-0 cotyledons infected with *Hpa* Emoy2, asexual or sexual reproduction of the avirulent pathogen was rarely observed (Figure 6a,b). Under our laboratory conditions, no more than two conidiophores or two oospores were usually seen (Figure 6a,b). No differences in resistance were observed in the transgenic lines expressing GFP-ATR13, HaRxLL495b-GFP or GFP-HaRxL77 (Figure 6a). However, a considerable increase in sexual reproduction of *Hpa* Emoy2 was observed in the transgenic lines expressing GFP-HaRxL17 (Figure 6a).

Differences in *Hpa* Emoy2 growth in Col-0 versus GFP-HaRxL17 lines were analysed in detail by trypan blue staining of infected cotyledons. Emoy2-infected Col-0 cotyledons showed development of few short hyphae in the epidermis and occasionally haustoria (Figure 6b). In contrast, GFP-HaRxL17 lines supported increased hyphal growth of *Hpa* Emoy2 (Figure 6c). This hyphae production may allow hyphae inter-twining, which is essential for sexual reproduction (Figure 6c). We also noted an increase in haustoria development (Figure 6c) in mesophyll cells, which resembled what was observed in the compatible interaction. To better understand the role of this effector during infection, we analysed haustoria formation in the GFP-HaRxL17 line infected with *Hpa* Emoy2 at the subcellular level. We identified encased haustoria at a late stage of the interaction (6 DAI) (Figure 6d). We then analysed the subcellular localization of HaRxL17 in *Hpa* Emoy2 haustorium-invaded mesophyll cells. *In vivo* confocal imaging revealed that HaRxL17 was strongly localized inside the encasement (Figure 6e), probably to the EHM. Thus, HaRxL17 is an effector that is strongly localized to the membrane around haustoria and increases the virulence of *Hpa* in both compatible and incompatible interactions.

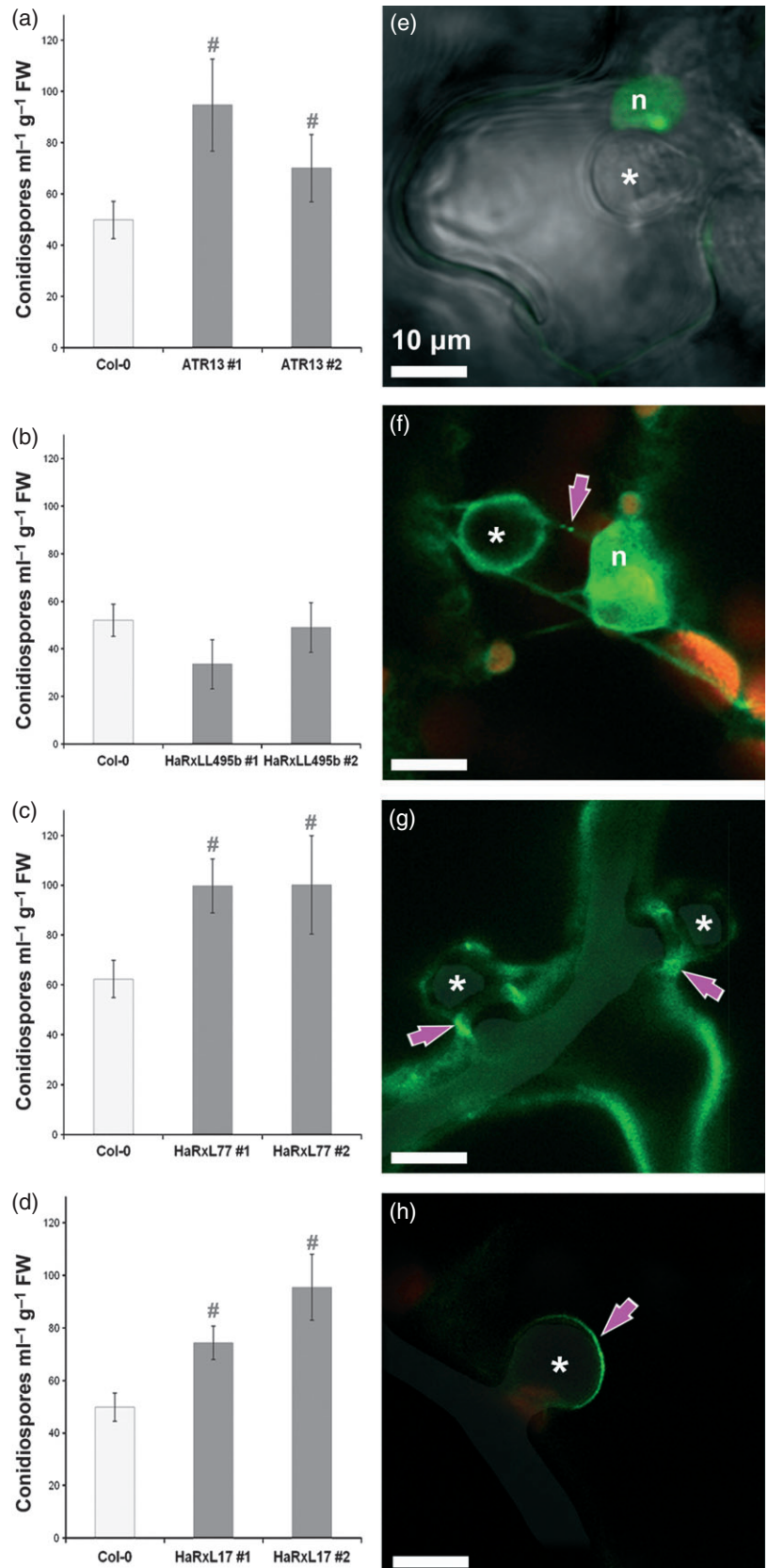
### DISCUSSION

The haustorium is a highly specialized feeding structure of phytopathogens of taxonomically distinct classes, including fungal powdery mildews, rusts and oomycetes. Here, we developed an *in vivo* cell biology approach in order to study the interaction between *Hpa* and Arabidopsis. We monitored changes to the subcellular architecture during *Hpa* infection in order to identify subcellular compartments that

**Figure 5.** HaRxL17 and HaRxL77 confer increased virulence to *Hpa* isolate Waco9.

(a–d) Monitoring of *Hpa* Waco9 sporulation in Col-0 wild-type (WT) or transgenic lines expressing individual HaRxLs at 5 DAI, expressed as the number of conidiospores per ml water per gram fresh weight (FW).

(e–h) Subcellular localization of GFP-tagged HaRxLs in transgenic lines 3 DAI with *Hpa* Waco9. The grey shadow (in g and h) indicates *Hpa* hyphae. (e) GFP-ATR13 localizes to the nucleolus in an infected mesophyll cell. (f) HaRxLL495b-GFP localizes to the ER around the haustoria and the nucleus in infected mesophyll cells. (g) GFP-HaRxL77 localizes to the PM in infected cells. (h) GFP-HaRxL17 localizes around the haustoria in an infected mesophyll cell. n, nucleus. The asterisks indicate haustoria, and pink arrows indicate the GFP-HaRxL significant localization. Scale bars = 10  $\mu$ m.





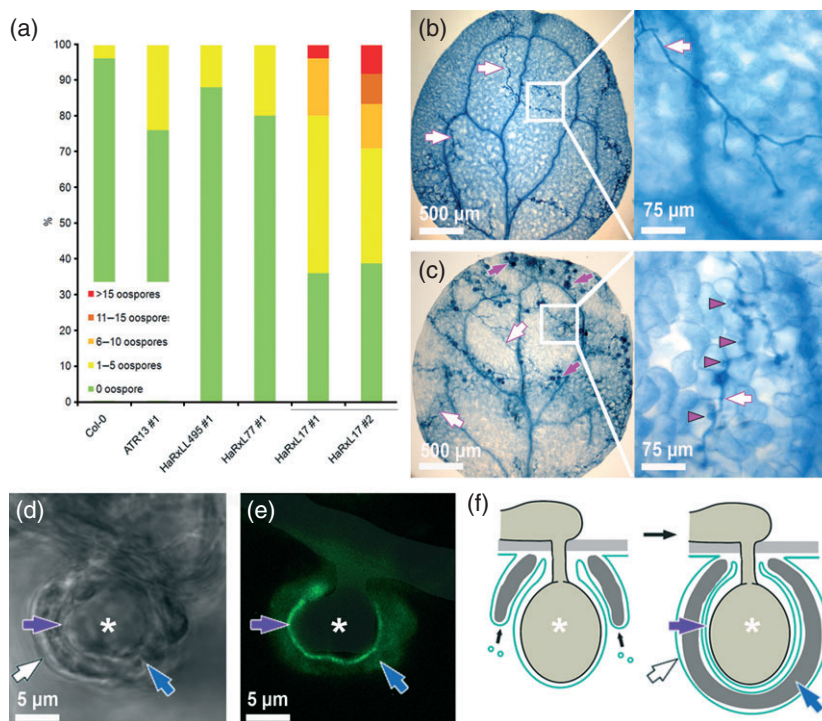


**Figure 6.** HaRxL17 promotes the sexual reproduction of *Hpa* Emoy2 in Arabidopsis Col-0 and localizes to the EHM.

(a) Oospore counts on cotyledons 6 DAI with *Hpa* Emoy2 for Col-0 WT and Col-0 stably expressing GFP-ATR13 (line 1), HaRxLL495b (line 1), GFP-HaRxL77 (line 1) or GFP-HaRxL17 (lines 1 and 2).

(b) General view and close-up view of *Hpa* Emoy2 growth at 6 DAI in Col-0 cotyledons (trypan blue staining). Open arrows indicate hyphae.

(c) General view and close-up of *Hpa* Emoy2 growth at 6 DAI in cotyledon of a GFP-HaRxL17 transgenic line (trypan blue staining). The white arrows indicate hyphae and pink arrowheads indicate haustoria visible in the mesophyll cell. Pink arrows indicate oospores.

(d) Morphological analyses of the haustoria in a GFP-HaRxL17 line infected with *Hpa* Emoy2. Bright-field image of a haustorium (asterisk) surrounded by encasement (blue arrow). The white arrow indicates the membrane surrounding the encased haustoria. The EHM is indicated by a purple arrow.

(e) HaRxL17 subcellular localization in a transgenic line expressing GFP-HaRxL17 during *Hpa* Emoy2 infection. Note that the GFP-HaRxL17 signal (purple arrow) strongly labels the EHM surrounding the haustorium (asterisk) inside the callose encasement (blue arrow).

(f) Proposed model for formation of haustorial encasements in *Hpa*-infected Arabidopsis mesophyll cells, modified from Meyer *et al.* (2009). The haustorium is indicated by an asterisk. The callose encasement is indicated by a blue arrow. The white arrow indicates the membrane around the encased haustorium. The EHM is indicated by a purple arrow. After full encasement of the haustorium, the EHM is trapped between the haustorium and the callose encasement.

play significant roles in defence responses. Further, we attempted to correlate this information with the subcellular localization of *Hpa* effector candidates and their functional role in compatible and incompatible interactions. Significantly, by identifying an effector that associates with the host tonoplast in non-infected cells and with the EHM in infected cells, this study has highlighted a possible relationship between vacuolar and defence-induced membranes that plays a role in establishment of a compatible interaction.

In order to identify the plant cell compartments targeted by pathogen effectors, several cell biology approaches have been used (Boevink *et al.*, 2011; Kemen *et al.*, 2011). As transformation systems are not yet available for most biotrophic pathogens, functional analysis of tagged effector proteins using heterologous systems remains one of the most promising options (Kelley *et al.*, 2010; Rafiqi *et al.*, 2010; Schornack *et al.*, 2010). In this study, we used fluores-

cent protein-tagged effectors that were either transiently or stably expressed in the plant cells. This approach allowed easy and rapid identification of promising pathogen effector candidates. However, we cannot exclude the possibility of any dominant-negative effects or interference by the GFP tag that could affect effector functions.

During the compatible interaction between *Hpa* and Arabidopsis, haustorium-invaded mesophyll cells undergo rearrangement. The plant cell nucleus stays close to the developing haustorium, presumably via movement through the actin cytoskeleton in infected mesophyll cells (Ketelaar *et al.*, 2002; Iwabuchi *et al.*, 2010). It is conceivable that the haustorium directly influences nuclear position in the cell to enhance delivery of effectors that compromise nuclear processes involved in defence. Alternatively, defence may be activated by hyphal penetration and haustorial development, although this is not sufficient to stop the growth of the pathogen. In this case, nuclear

proximity to the haustorium maximizes the efficiency of delivery of anti-microbial transcripts and proteins to the intruding structure. The plant ER and Golgi surround developing haustoria, suggesting that production and secretion of plant materials are activated around the haustoria. We showed that, in contrast to the exclusion of PM markers around haustoria, the tonoplast is in close proximity to the EHM. *In vivo* time-lapse imaging of  $\gamma$ -TIP-GFP-labelled tonoplast membrane revealed the presence of numerous bulbs in *Hpa*-infected cells. Extensive examination by fluorescence and electron microscopy demonstrated that the bulbs are projections of cytoplasm, often consisting of two membranes (Saito *et al.*, 2002). The outer and inner membranes, as well as the limiting vacuolar membrane, appear to be connected (Saito *et al.*, 2002). Even though the role of these bulbs remains unclear (Saito *et al.*, 2002, 2011; Escobar *et al.*, 2003; Hicks *et al.*, 2004; Beebo *et al.*, 2009), it has been suggested that, if some vacuoles are not easily fused, double-membrane structures (bulbs) may be left behind for some time (Saito *et al.*, 2002; Beebo *et al.*, 2009). As bulbs accumulate in haustorium-invaded mesophyll cells, we speculate that turnover of the vacuolar membrane in mesophyll cells may be disturbed in the presence of the pathogen. The high-affinity phosphate transporter PT1 also localized to bulb structures (Escobar *et al.*, 2003). Thus, it is plausible that bulbs enable re-mobilization of phosphate from the central vacuole to the haustoria.

#### Why do many *Hpa* RxLR effectors target the plant cell nucleus?

Increasing evidence suggests that the plant cell nucleus is one of the main targets for pathogen effectors. Recent studies that examined interactions between plants and bacterial pathogens found that effectors are probably targeting the host nucleus in order to re-program the plant cell transcriptional machinery, suppress the plant immune response and subsequently promote pathogen virulence (Kay and Bonas, 2009; Boch and Bonas, 2010). Recent advances in functional analysis of oomycete effectors from *P. infestans* confirmed that CRINKLER (CRN) effectors target the nucleus (Schornack *et al.*, 2010). The authors showed that inhibition of CRN8 nuclear accumulation prevented cell death, and thus that CRN8 nuclear localization is required for cell-death induction. In the present study, the survey of the *in planta* subcellular localization of one third of the predicted HaRxLs revealed that a large majority (66%) targeted the plant cell nucleus. In contrast with effectors from bacterial pathogens, canonical nuclear localization signals are rarely predicted in the sequence of these oomycete effectors. Thus, oomycete effectors may have evolved other ways that allow them to target the plant cell nucleus, perhaps by association with endogenous host protein(s).

Twenty-one per cent of the HaRxLs tested (merging the strictly nucleolar and the nucleolar-cytoplasmic), including ATR13<sup>Maks9</sup> and ATR13<sup>Emoy2</sup>, localized to the host nucleolus. Of all plant pathogens, only secreted proteins from cyst nematodes have been reported to target the plant nucleolus (Tytgat *et al.*, 2005; Elling *et al.*, 2009). The main functions of the nucleolus lie in transcription of ribosomal RNA gene units, processing and modification of precursor rRNA, and ribosomal subunit assembly (Brown *et al.*, 2005; Raska *et al.*, 2006). We hypothesize that *Hpa* hijacks the plant cell transcriptional machinery, acting on ribosome biogenesis and thus on protein translation in order to prevent *de novo* induction of defence responses. In addition, the nucleolus has been implicated in a variety of other functions, including biogenesis, transport, splicing of RNAs and transcriptional gene silencing (Pontes and Pikaard, 2008; Rodor *et al.*, 2010). Thus, these additional processes could be the target of nucleolar-localized HaRxLs. We found specific sub-nuclear localizations for some HaRxLs that resemble the localization of already characterized Arabidopsis nucleolar proteins. For example, the nucleolar cap-like structures observed using GFP-HaRxL36 *in planta* resemble the localization of the Prp19-like U-box proteins, which are associated with the MOS4-associated complexes that are involved in plant innate immunity (Monaghan *et al.*, 2009). Thus, detailed functional analysis of nucleolar-localized HaRxLs and identification of their plant targets may identify unknown processes that are essential for *Hpa* virulence.

#### Why do *Hpa* RxLR effectors target the plant plasma membrane?

The first level of microbe recognition in plants is performed by membrane proteins termed pattern recognition receptors (PRRs), which perceive molecular signatures characteristic of a whole class of microbes, termed pathogen-associated molecular patterns (PAMPs). To infect plants successfully, pathogens must overcome PAMP-triggered immunity (PTI). Several recent studies clearly showed that one strategy to do so is to directly target PRRs and their associated proteins by the action of virulence effectors (Robert-Seilanianantz *et al.*, 2006; Thieme *et al.*, 2007; Downen *et al.*, 2009; Wu *et al.*, 2011). In contrast with bacterial effectors, nothing is known about membrane-localized effectors of eukaryotic phytopathogens. Recently, the receptor-like kinase SERK3/BAK1 was shown to be required for basal resistance against *P. infestans* in *N. benthamiana* (Chaparro-Garcia *et al.*, 2011), indicating that some of the defence mechanisms employed by host cells in response to bacteria overlap with those induced in response to oomycetes. In addition, recent data showed that PAMP pre-elicitation impairs *Hpa* growth (and reproduction), indicating that *Hpa* must counteract PTI responses in order to promote virulence (Fabro *et al.*, 2011). In the present study, we identified three Emoy2 HaRxLs and one Noco2 HaRxL that target the plant PM. Arabidopsis lines

expressing the PM-localized HaRxL77 were more susceptible to *Hpa* than Col-0, indicating that HaRxL77 increases *Hpa* virulence during a compatible interaction. The localization of HaRxL77 at the PM suggests that this effector may act on PTI responses during pathogen growth. Recent evidence also suggested that vesicle trafficking is an important component of PTI (Frei dit Frey and Robatzek, 2009). Thus, we hypothesize that the PM-localized HaRxL77 may prevent exocytosis of defence components or endocytosis of PRR in order to dampen or regulate PTI responses. Bozkurt *et al.* (2011) showed that the *P. infestans* AVRblb2 effector interferes with secretion of host cysteine protease C14, thus reducing its contribution to defence.

#### How can the study of membrane-localized HaRxLs help to understand EHM ontogenesis?

Live-cell imaging revealed that GFP–HaRxL17 localized to the EHM at a late stage of infection between *Hpa* Emoy2 and Col-0. Previous searches for EHM-resident proteins had limited success. In the present study, however, live-cell imaging showed that RPW8.2 localized into vesicle-like bodies surrounding the *Hpa* haustorium during the early stage of infection, but was absent from the EHM. In mature haustoria, RPW8.2 localized to callose-rich encasements, as described for haustoria from powdery mildew. Ultrastructural characterization of the haustorial interface in the *Golovinomyces orontii*/Arabidopsis interaction confirmed the recruitment of RPW8.2 to the EHM of mature haustoria (Micali *et al.*, 2011). As no EHM-localized proteins have been identified at the EHM of young haustoria, the mechanism by which the EHM is formed remains elusive, preventing complete understanding of compatible interactions between haustoria-forming pathogens and their hosts (Koh and Somerville, 2006). Recently, Bozkurt *et al.* (2011) showed that GFP:AVRblb2 fusion protein preferentially accumulated around *P. infestans* haustoria.

Ultrastructural studies of haustorium-invaded cells have identified that the EHM is proximal to the tonoplast, sandwiching a very thin layer of host-cell cytoplasm (approximately 0.1 µm) between the EHM and the tonoplast (Chou, 1970; Mims *et al.*, 2004). Using live-cell imaging, we detailed the behaviour of the tonoplast over a time course of *Hpa* infection, and showed that the tonoplast intrinsic protein  $\gamma$ -TIP–GFP strongly labelled membranes within the EHM in young haustoria. The EHM and the tonoplast are too close in infected cells to distinguish between them using light microscopy, and thus higher-resolution techniques are required to determine whether or not this marker labels the EHM. The difference in localization of HaRxL17 in infected cells (EHM) and uninfected cells (tonoplast), and the changes to the vacuolar sub-structure induced by infection, indicate that vacuole-associated membranes are highly dynamic during haustoria formation. Indeed, the role that the tonoplast plays in haustoria formation and secretion

of defence compounds requires further examination. The association of GFP–HaRxL17 with the EHM of mature haustoria can be exploited to further investigate the composition of this particular membrane. Biochemical analysis of plants expressing GFP-tagged HaRxL17 during infection with *Hpa* may allow us to identify plant-interacting proteins that localize to the EHM and to understand the plant cell vesicle trafficking that allows formation of the final membrane layer separating the host cell from its invader. In addition, localization of HaRxL17 in the native system at the cellular and subcellular level using immunocytological techniques (Kemen *et al.*, 2011) will help us to understand the function of this effector during haustoria ontogenesis.

Characterization of nuclear and membrane-localized HaRxL functions will be critical for understanding the basis of plant pathogenesis. Further understanding of the cell biology and compartmentalization of signalling and metabolic processes during plant–pathogen interactions will highlight the mechanisms employed in the fight against infection.

## EXPERIMENTAL PROCEDURES

### Cloning of HaRxLs

To produce the effector candidate collection, primers for amplification were designed from the *Hpa* Emoy2 genome version 8.3 (Baxter *et al.*, 2011). The HaRxL sequences are available in Fabro *et al.* (2011). Selected HaRxLs were amplified from the signal peptide cleavage site to the stop codon using genomic DNA extracted from conidiospores of *Hpa* Emoy2 and Accuprime Pfx proof-reading polymerase (Invitrogen, <http://www.invitrogen.com/>) under standard PCR conditions. The PCR fragment was inserted into the pENTR donor vector (Invitrogen) and then into plant expression vectors pK7WGF2, pK7FWG2, pH7WGR2 or pH7WGY2 using Gateway technology (Invitrogen). The constructs were sequenced by the Genome Analysis Centre in Norwich (UK).

### Bioinformatic analysis

PSORTII (<http://psort.hgc.jp/form2.html>) was used for prediction of the subcellular localization of the HaRxLs and Coil ([http://www.ch.embnet.org/software/COILS\\_form.html](http://www.ch.embnet.org/software/COILS_form.html)), TMHMM version 2.0 (<http://www.cbs.dtu.dk/services/TMHMM/>), PFAM (<http://pfam.sanger.ac.uk/>) and Prosite (<http://prosite.expasy.org/>) were used to check the presence of known conserved protein domains. The predicted nuclear-localization signal was determined using WolfPsort (<http://wolfsort.org/>) and NLStradamus (<http://www.moseslab.csb.utoronto.ca/NLStradamus/>).

### Expression pattern analysis

The expression pattern of HaRxL candidates was determined using cDNA for Illumina sequencing (from tissue at 3 and 7 days post-infection) (Fabro *et al.*, 2011). For semi-quantitative RT-PCR, 50 ng of total RNA was used and amplified with an initial denaturation step at 95°C for 3 min followed by 25 cycles of 45 sec at 94°C, 30 sec at 55°C and 72°C for 30 sec. In the last cycle, a final elongation step at 72°C for 5 min was added. PCR products were separated on 1.5% TAE agarose gels. The *RPL4* gene was used to control.



### Transient and stable expression *in planta*

For *in planta* expression of the fluorescent protein-tagged HaRXLs, *A. tumefaciens* strains GV3101 and GV3103 were used to deliver transgenes into *N. benthamiana* leaves (Caillaud *et al.*, 2009). Protein stability was assessed using Western blotting as described by Schornack *et al.* (2010). For stable expression *in planta* of selected candidates, Col-0 Arabidopsis plants were transformed using the dipping method (Clough and Bent, 1998) and selected on MS medium per 0.7% agar plates containing 50 µg ml<sup>-1</sup> kanamycin. Transformed plants were transferred to soil and seeds were collected. Ten transformed plants were analysed for each construct. T<sub>3</sub> homozygous plants were used for *in vivo* confocal microscopy and pathogen assays. For fractionation analysis, two independent Arabidopsis lines expressing GFP-HaRXL17 or free GFP were used in two independent experiments. Fractionation was performed as described by Boyes *et al.* (1998).

### Pathogen assays

For infection, 10-day-old plants were spray-inoculated to run-off using a spore suspension of  $5 \times 10^4$  conidiospores per ml. Plants were kept in a growth cabinet at 16°C for 6 days with a 10 h photoperiod. To evaluate conidiospore production, ten pools of two plants for each Arabidopsis line were harvested in 1 ml of water. After vortexing, the amount of conidiospores released was determined using a haemocytometer as described by Robert-Seilaniantz *et al.* (2011). Statistical analyses were performed using ANOVA for three independent experiments.

To evaluate hyphae growth and oospore production, infected cotyledons were stained with trypan blue. For *Hpa* Emoy2 infection in Col-0 and transgenic lines, the number of oospores per cotyledons was manually scored by observing the abaxial and adaxial surfaces of each cotyledon of 30 plants per line. For imaging of *Hpa* Emoy2 development in the cotyledons, the samples were observed using a Leica DM R fluorescence microscope (<http://www.leica.com/>). Photographs were taken using a Leica DFC 300 FX digital camera.

### Confocal microscopy

For determination of the subcellular localization of the HaRXLs in *N. benthamiana*, cut leaf samples were mounted in water and analysed on a Leica DM6000B/TCS SP5 confocal microscope using the following excitation wavelengths: GFP, 488 nm; YFP, 516 nm; RFP, 561 nm. For *in vivo* localization in Arabidopsis transgenic lines, 10-day-old infected seedlings were mounted in water and analysed on a Leica DM6000B/TCS SP5 confocal microscope using the following excitation wavelengths: CFP, 458 nm; GFP, 488 nm; RFP, 561 nm. The HaRXL sub-nuclear localizations were named according to the nomenclature in the Arabidopsis nucleolar protein database at <http://bioinf.scri.sari.ac.uk/cgi-bin/atnodb/home>.

### ACKNOWLEDGEMENTS

We thank Peter Shaw's laboratory (John Innes Centre, Norwich, UK) for the generous gift of H2A-GFP Arabidopsis seeds. We thank Jordi Chan (John Innes Centre, Norwich, UK) and Volker Lipka (Albrecht-von-Haller, Göttingen, Germany) for access to Arabidopsis fluorescent markers, and Grant Calder (John Innes Centre, Norwich, UK) for his technical support. We thank Matthew Smoker (TSL, Norwich, UK) and Jodie Pike (TSL, Norwich, UK) for stable transformation of Arabidopsis. We thank Fabio Galeotti (UEA, Norwich, UK) for his help with statistics. We thank Freddy Boutrot (TSL, Norwich, UK)

and Tolga Bozkurt (TSL, Norwich, UK) for their help with fractionation analysis. We would also like to thank Christine Faulkner (John Innes Centre, Norwich, UK) Ali Pendle (John Innes Centre, Norwich, UK), Silke Robatzek (TSL, Norwich, UK) and Valérie Nicaise (TSL, Norwich, UK) for fruitful discussions and their help with the manuscript. We thank Sophien Kamoun, Sebastian Schornack and Tolga Bozkurt for early sight of their discovery of focal recruitment of Avr-blb2 to *P. infestans* haustoria, and for helpful discussion to improve the manuscript. This work was supported by long-term fellowships EMBO ALTF 614 and Marie Curie FP7-PEOPLE-2009-IEF to M.C.C., Biotechnology and Biological Sciences Research Council grant G015066 to J.B. and the Gatsby Foundation. This paper is dedicated to Madeleine and Jean-Pierre Caillaud.

### SUPPORTING INFORMATION

Additional Supporting Information may be found in the online version of this article:

**Figure S1.** *In vivo* localization of plant cell compartments in *Hpa* Waco9 haustorium-invaded mesophyll cells.

**Figure S2.** *In vivo* localization of PEN1 and RPW8.2 during *Hpa* haustorium ontogenesis in Arabidopsis mesophyll cells.

**Figure S3.** Immunoblot analysis of GFP- and RFP-tagged RxLR effector candidates expressed transiently in *N. benthamiana*.

**Figure S4.** Subcellular localization screening of HaRXLs.

**Figure S5.** Subcellular localization screening of HaRXLs.

**Figure S6.** Expression pattern of selected HaRXLs during a time course of *Hpa* infection in Arabidopsis.

**Figure S7.** Western blot analysis of Arabidopsis lines expressing GFP-tagged HaRXLs.

**Figure S8.** Subcellular localizations of GFP-tagged HaRXLs stably expressed in Arabidopsis.

**Figure S9.** Fractionation analysis of Arabidopsis lines expressing GFP-HaRXL17.

**Table S1.** HaRXL subcellular localization screening *in planta*.

**Video Clips S1 and S2.** *In vivo* dynamics of the tonoplast in *Hpa* Waco9 haustorium-invaded mesophyll cells.

**Video Clip S3.** *In vivo* dynamic of the subcellular localization of GFP-HaRXL17 *in planta*.

Please note: As a service to our authors and readers, this journal provides supporting information supplied by the authors. Such materials are peer-reviewed and may be re-organized for online delivery, but are not copy-edited or typeset. Technical support issues arising from supporting information (other than missing files) should be addressed to the authors.

### REFERENCES

- Allen, R.L., Bittner-Eddy, P.D., Grenville-Briggs, L.J., Meitz, J.C., Rehmany, A.P., Rose, L.E. and Beynon, J.L. (2004) Host-parasite coevolutionary conflict between Arabidopsis and downy mildew. *Science*, **306**, 1957–1960.
- Bailey, K., Çevik, V., Holton, N.J. *et al.* (2011) Molecular cloning of ATR5<sup>Emoy2</sup> from *Hyaloperonospora arabidopsidis*, an avirulence determinant that triggers RPP5-mediated defense in Arabidopsis. *Mol. Plant Microbe Interact.* **24**, 827–838.
- Baxter, L., Tripathy, S., Ishaque, N. *et al.* (2010) Signatures of adaptation to obligate biotrophy in the *Hyaloperonospora arabidopsidis* genome. *Science*, **330**, 1549–1551.
- Beebo, A., Thomas, D., Der, C., Sanchez, L., Leborgne-Castel, N., Marty, F., Schoefs, B. and Bouhidel, K. (2009) Life with and without AtTIP1;1, an Arabidopsis aquaporin preferentially localized in the apposing tonoplasts of adjacent vacuoles. *Plant Mol. Biol.* **70**, 193–209.
- van der Biezen, E.A., Freddie, C.T., Kahn, K., Parker, J.E. and Jones, J.D. (2002) Arabidopsis RPP4 is a member of the RPP5 multigene family of TIR-NB-LRR genes and confers downy mildew resistance through multiple signalling components. *Plant J.* **29**, 439–451.

- Birch, P.R., Rehmany, A.P., Pritchard, L., Kamoun, S. and Beynon, J.L. (2006) Trafficking arms: oomycete effectors enter host plant cells. *Trends Microbiol.* **14**, 8–11.
- Boch, J. and Bonas, U. (2010) *Xanthomonas* AvrBs3 family-type III effectors: discovery and function. *Annu. Rev. Phytopathol.* **48**, 419–436.
- Boevink, P.C., Birch, P.R. and Whisson, S.C. (2011) Imaging fluorescently tagged *Phytophthora* effector proteins inside infected plant tissue. *Methods Mol. Biol.* **712**, 195–209.
- Bos, J.I., Kanneganti, T.D., Young, C., Cakir, C., Huitema, E., Win, J., Armstrong, M.R., Birch, P.R. and Kamoun, S. (2006) The C-terminal half of *Phytophthora infestans* RXLR effector AVR3a is sufficient to trigger R3a-mediated hypersensitivity and suppress INF1-induced cell death in *Nicotiana benthamiana*. *Plant J.* **48**, 165–176.
- Bos, J.I., Armstrong, M.R., Gilroy, E.M. et al. (2010) *Phytophthora infestans* effector AVR3a is essential for virulence and manipulates plant immunity by stabilizing host E3 ligase CMPG1. *Proc. Natl Acad. Sci. USA*, **107**, 9909–9914.
- Boyes, D.C., Nam, J. and Dangel, J.L. (1998) The *Arabidopsis thaliana* RPM1 disease resistance gene product is a peripheral plasma membrane protein that is degraded coincident with the hypersensitive response. *Proc. Natl Acad. Sci. USA*, **95**, 15849–15854.
- Bozkurt, T.O., Schornack, S., Win, J., Shindo, T., Ilyas, M., Oliva, R., Cano, L.M., Jones, A.M., Huitema, A.M., van der Hoorn, R.A. and Kamoun, S. (in press) *Phytophthora infestans* effector AVRblb2 prevents secretion of a plant immune protease at the haustorial interface. *Proc Natl Acad Sci USA*.
- Brown, J.W., Shaw, P.J., Shaw, P. and Marshall, D.F. (2005) Arabidopsis nucleolar protein database (AtNoPDB). *Nucleic Acids Res.* **33**, D633–D636.
- Bushnell, W.R. (1972) Physiology of fungal haustoria. *Annu. Rev. Phytopathol.* **10**, 151–176.
- Cabral, A., Stassen, J.H., Seidl, M.F., Bautor, J., Parker, J.E. and Van den Ackerveken, G. (2011) Identification of *Hyaloperonospora arabidopsidis* transcript sequences expressed during infection reveals isolate-specific effectors. *PLoS One*, **6**, e19328.
- Caillaud, M.C., Paganelli, L., Lecomte, P., Deslandes, L., Quentin, M., Pecrix, Y., Le Bris, M., Marfaing, N., Abad, P. and Favery, B. (2009) Spindle assembly checkpoint protein dynamics reveal conserved and unsuspected roles in plant cell division. *PLoS One*, **4**, e6757.
- Chaparro-Garcia, A., Wilkinson, R.C., Gimenez-Ibanez, S., Findlay, K., Coffey, M.D., Zipfel, C., Rathjen, J.P., Kamoun, S. and Schornack, S. (2011) The receptor-like kinase SERK3/BAK1 is required for basal resistance against the late blight pathogen *Phytophthora infestans* in *Nicotiana benthamiana*. *PLoS One*, **6**, e16608.
- Chou, C.K. (1970) An electron-microscope study of host penetration and early stages of haustorium formation of *Peronospora parasitica* (Fr.) Tul. on cabbage cotyledons. *Ann. Bot.* **34**, 189–204.
- Clough, S.J. and Bent, A.F. (1998) Floral dip: a simplified method for *Agrobacterium*-mediated transformation of *Arabidopsis thaliana*. *Plant J.* **16**, 735–743.
- Collins, N.C., Thordal-Christensen, H., Lipka, V. et al. (2003) SNARE-protein-mediated disease resistance at the plant cell wall. *Nature*, **425**, 973–977.
- De Wit, P.J., Mehrabi, R., Van den Burg, H.A. and Stergiopoulos, I. (2009) Fungal effector proteins: past, present and future. *Mol. Plant Pathol.* **10**, 735–747.
- Dou, D., Kale, S.D., Wang, X., Jiang, R.H., Bruce, N.A., Arredondo, F.D., Zhang, X. and Tyler, B.M. (2008) RXLR-mediated entry of *Phytophthora sojae* effector Avr1b into soybean cells does not require pathogen-encoded machinery. *Plant Cell*, **20**, 1930–1947.
- Downen, R.H., Engel, J.L., Shao, F., Ecker, J.R. and Dixon, J.E. (2009) A family of bacterial cysteine protease type III effectors utilizes acylation-dependent and -independent strategies to localize to plasma membranes. *J. Biol. Chem.* **284**, 15867–15879.
- Elling, A.A., Mitreva, M., Gai, X., Martin, J., Recknor, J., Davis, E.L., Hussey, R.S., Nettleton, D., McCarter, J.P. and Baum, T.J. (2009) Sequence mining and transcript profiling to explore cyst nematode parasitism. *BMC Genomics*, **10**, 58.
- Ellis, J.G., Rafiqi, M., Gan, P., Chakrabarti, A. and Dodds, P.N. (2009) Recent progress in discovery and functional analysis of effector proteins of fungal and oomycete plant pathogens. *Curr. Opin. Plant Biol.* **12**, 399–405.
- Escobar, N.M., Haupt, S., Thow, G., Boevink, P., Chapman, S. and Oparka, K. (2003) High-throughput viral expression of cDNA-green fluorescent protein fusions reveals novel subcellular addresses and identifies unique proteins that interact with plasmodesmata. *Plant Cell*, **15**, 1507–1523.
- Fabro, G., Steinbrenner, J., Coates, M. et al. (2011) Multiple effectors from the oomycete pathogen *Hyaloperonospora arabidopsidis* suppress host plant immunity. *PLoS Pathog.* **7**, e1002348.
- Frei dit Frey, N. and Robatzek, S. (2009) Trafficking vesicles: pro or contra pathogens? *Curr. Opin. Plant Biol.* **12**, 437–443.
- Geldner, N., Denervaud-Tendon, V., Hyman, D.L., Mayer, U., Stierhof, Y.D. and Chory, J. (2009) Rapid, combinatorial analysis of membrane compartments in intact plants with a multicolor marker set. *Plant J.* **59**, 169–178.
- Genre, A., Chabaud, M., Timmers, T., Bonfante, P. and Barker, D.G. (2005) Arbuscular mycorrhizal fungi elicit a novel intracellular apparatus in *Medicago truncatula* root epidermal cells before infection. *Plant Cell*, **17**, 3489–3499.
- Gilroy, E.M., Breen, S., Whisson, S.C. et al. (2011) Presence/absence, differential expression and sequence polymorphisms between PiAVR2 and PiAVR2-like in *Phytophthora infestans* determine virulence on R2 plants. *New Phytol.* **191**, 763–776.
- Gurlebeck, D., Thieme, F. and Bonas, U. (2006) Type III effector proteins from the plant pathogen *Xanthomonas* and their role in the interaction with the host plant. *J. Plant Physiol.* **163**, 233–255.
- Haverkort, A.J., Boonekamp, P.M., Hutten, R., Jacobsen, E., Lotz, L.A.P., Kessel, G.J.T., Visser, R.G.F. and van der Vossen, E.A.G. (2008) Societal costs of late blight in potato and prospects of durable resistance through cisgenic modification. *Potato Res.* **51**, 47–57.
- Hicks, G.R., Rojo, E., Hong, S., Carter, D.G. and Raikhel, N.V. (2004) Germinating pollen has tubular vacuoles, displays highly dynamic vacuole biogenesis, and requires VACUOLESS1 for proper function. *Plant Physiol.* **134**, 1227–1239.
- Hogenhout, S.A., Van der Hoorn, R.A., Terauchi, R. and Kamoun, S. (2009) Emerging concepts in effector biology of plant-associated organisms. *Mol. Plant Microbe Interact.* **22**, 115–122.
- Hok, S., Attard, A. and Keller, H. (2010) Getting the most from the host: how pathogens force plants to cooperate in disease. *Mol. Plant Microbe Interact.* **23**, 1253–1259.
- Howard, R.J. and Valent, B. (1996) Breaking and entering: host penetration by the fungal rice blast pathogen *Magnaporthe grisea*. *Annu. Rev. Microbiol.* **50**, 491–512.
- Huckelhoven, R. (2007) Transport and secretion in plant-microbe interactions. *Curr. Opin. Plant Biol.* **10**, 573–579.
- Iwabuchi, K., Minamino, R. and Takagi, S. (2010) Actin reorganization underlies phototropin-dependent positioning of nuclei in Arabidopsis leaf cells. *Plant Physiol.* **152**, 1309–1319.
- Jiang, R.H., Tripathy, S., Govers, F. and Tyler, B.M. (2008) RXLR effector reservoir in two *Phytophthora* species is dominated by a single rapidly evolving superfamily with more than 700 members. *Proc. Natl Acad. Sci. USA*, **105**, 4874–4879.
- Kalde, M., Nuhse, T.S., Findlay, K. and Peck, S.C. (2007) The syntaxin SYP132 contributes to plant resistance against bacteria and secretion of pathogenesis-related protein 1. *Proc. Natl Acad. Sci. USA*, **104**, 11850–11855.
- Kale, S.D., Gu, B., Capelluto, D.G. et al. (2010) External lipid PI3P mediates entry of eukaryotic pathogen effectors into plant and animal host cells. *Cell*, **142**, 284–295.
- Kamoun, S. (2007) Groovy times: filamentous pathogen effectors revealed. *Curr. Opin. Plant Biol.* **10**, 358–365.
- Kay, S. and Bonas, U. (2009) How *Xanthomonas* type III effectors manipulate the host plant. *Curr. Opin. Microbiol.* **12**, 37–43.
- Kelley, B.S., Lee, S.J., Damasceno, C.M., Chakravarthy, S., Kim, B.D., Martin, G.B. and Rose, J.K. (2010) A secreted effector protein (SNE1) from *Phytophthora infestans* is a broadly acting suppressor of programmed cell death. *Plant J.* **62**, 357–366.
- Kemen, E., Kemen, A.C., Rafiqi, M., Hempel, U., Mendgen, K., Hahn, M. and Voegelé, R.T. (2005) Identification of a protein from rust fungi transferred from haustoria into infected plant cells. *Mol. Plant Microbe Interact.* **18**, 1130–1139.
- Kemen, E., Mendgen, K. and Voegelé, R.T. (2011) Immunolocalization of pathogen effectors. *Methods Mol. Biol.* **712**, 211–225.
- Ketelaar, T., Faivre-Moskalenko, C., Esseling, J.J., de Ruijter, N.C., Grierson, C.S., Dogterom, M. and Emons, A.M. (2002) Positioning of nuclei in Ara-

- bidopsis root hairs: an actin-regulated process of tip growth. *Plant Cell*, **14**, 2941–2955.
- Koh, S. and Somerville, S. (2006) Show and tell: cell biology of pathogen invasion. *Curr. Opin. Plant Biol.* **9**, 406–413.
- Koh, S., Andre, A., Edwards, H., Ehrhardt, D. and Somerville, S. (2005) *Arabidopsis thaliana* subcellular responses to compatible *Erysiphe cichoracearum* infections. *Plant J.* **44**, 516–529.
- Meyer, D., Pajonk, S., Micali, C., O'Connell, R. and Schulze-Lefert, P. (2009) Extracellular transport and integration of plant secretory proteins into pathogen-induced cell wall compartments. *Plant J.* **57**, 986–999.
- Micali, C.O., Neumann, U., Grunewald, D., Panstruga, R. and O'Connell, R. (2011) Biogenesis of a specialized plant-fungal interface during host cell internalization of *Golovinomyces orontii* haustoria. *Cell Microbiol.* **13**, 210–226.
- Mims, C.W., Richardson, E.A., Holt, B.F. III and Dangl, J.L. (2004) Ultrastructure of the host-pathogen interface in *Arabidopsis thaliana* leaves infected by the downy mildew *Hyaloperonospora parasitica*. *Can. J. Bot.* **82**, 1001–1008.
- Monaghan, J., Xu, F., Gao, M., Zhao, Q., Palma, K., Long, C., Chen, S., Zhang, Y. and Li, X. (2009) Two Prp19-like U-box proteins in the MOS4-associated complex play redundant roles in plant innate immunity. *PLoS Pathog.* **5**, e1000526.
- Nelson, B.K., Cai, X. and Nebenfuhr, A. (2007) A multicolored set of in vivo organelle markers for co-localization studies in Arabidopsis and other plants. *Plant J.* **51**, 1126–1136.
- Nomura, K., Mecey, C., Lee, Y.N., Imboden, L.A., Chang, J.H. and He, S.Y. (2011) Effector-triggered immunity blocks pathogen degradation of an immunity-associated vesicle traffic regulator in Arabidopsis. *Proc. Natl Acad. Sci. USA*, **108**, 10774–10779.
- Pang, K.M., Lee, E. and Knecht, D.A. (1998) Use of a fusion protein between GFP and an actin-binding domain to visualize transient filamentous-actin structures. *Curr. Biol.* **8**, 405–408.
- Pontes, O. and Pikaard, C.S. (2008) siRNA and miRNA processing: new functions for Cajal bodies. *Curr. Opin. Genet. Dev.* **18**, 197–203.
- van Poppel, P.M., Guo, J., van de Vondervoort, P.J., Jung, M.W., Birch, P.R., Whisson, S.C. and Govers, F. (2008) The *Phytophthora infestans* avirulence gene *Avr4* encodes an RXLR-deER effector. *Mol. Plant Microbe Interact.* **21**, 1460–1470.
- Poueymiro, M. and Genin, S. (2009) Secreted proteins from *Ralstonia solanacearum*: a hundred tricks to kill a plant. *Curr. Opin. Microbiol.* **12**, 44–52.
- Rafiqi, M., Gan, P.H., Ravensdale, M., Lawrence, G.J., Ellis, J.G., Jones, D.A., Hardham, A.R. and Dodds, P.N. (2010) Internalization of flax rust avirulence proteins into flax and tobacco cells can occur in the absence of the pathogen. *Plant Cell*, **22**, 2017–2032.
- Raska, I., Shaw, P.J. and Cmarko, D. (2006) Structure and function of the nucleolus in the spotlight. *Curr. Opin. Cell Biol.* **18**, 325–334.
- Rehmany, A.P., Gordon, A., Rose, L.E., Allen, R.L., Armstrong, M.R., Whisson, S.C., Kamoun, S., Tyler, B.M., Birch, P.R. and Beynon, J.L. (2005) Differential recognition of highly divergent downy mildew avirulence gene alleles by *RPP1* resistance genes from two Arabidopsis lines. *Plant Cell*, **17**, 1839–1850.
- Robatzek, S. (2007) Vesicle trafficking in plant immune responses. *Cell Microbiol.* **9**, 1–8.
- Robert-Seilaniantz, A., Shan, L., Zhou, J.M. and Tang, X. (2006) The *Pseudomonas syringae* pv. *tomato* DC3000 type III effector HopF2 has a putative myristoylation site required for its avirulence and virulence functions. *Mol. Plant Microbe Interact.* **19**, 130–138.
- Robert-Seilaniantz, A., Maclean, D., Jikumaru, Y., Hill, L., Yamaguchi, S., Kamiya, Y. and Jones, J.D. (2011) The microRNA miR393 redirects secondary metabolite biosynthesis away from camalexin and towards glucosinolates. *Plant J.* **67**, 218–231.
- Rodor, J., Letelier, I., Holuigue, L. and Echeverria, M. (2010) Nucleolar RNPs: from genes to functional snoRNAs in plants. *Biochem. Soc. Trans.* **38**, 672–676.
- Saito, C., Ueda, T., Abe, H., Wada, Y., Kuroiwa, T., Hisada, A., Furuya, M. and Nakano, A. (2002) A complex and mobile structure forms a distinct sub-region within the continuous vacuolar membrane in young cotyledons of Arabidopsis. *Plant J.* **29**, 245–255.
- Saito, C., Uemura, T., Awai, C., Tominaga, M., Ebine, K., Ito, J., Ueda, T., Abe, H., Morita, M.T., Tasaka, M. and Nakano, A. (2011) The occurrence of 'bulbs', a complex configuration of the vacuolar membrane, is affected by mutations of vacuolar SNARE and phospholipase in Arabidopsis. *Plant J.* **68**, 64–73.
- Schornack, S., van Damme, M., Bozkurt, T.O., Cano, L.M., Smoker, M., Thines, M., Gaulin, E., Kamoun, S. and Huitema, E. (2010) Ancient class of translocated oomycete effectors targets the host nucleus. *Proc. Natl Acad. Sci. USA*, **107**, 17421–17426.
- Singh, R.P., Hodson, D.P., Huerta-Espino, J., Jin, Y., Bhavani, S., Njau, P., Herrera-Foessel, S., Singh, P.K., Singh, S. and Govindan, V. (2011) The emergence of Ug99 races of the stem rust fungus is a threat to world wheat production. *Annu. Rev. Phytopathol.* **49**, 465–481.
- Sohn, K.H., Lei, R., Nemri, A. and Jones, J.D. (2007) The downy mildew effector proteins ATR1 and ATR13 promote disease susceptibility in *Arabidopsis thaliana*. *Plant Cell*, **19**, 4077–4090.
- Takemoto, D., Jones, D.A. and Hardham, A.R. (2003) GFP-tagging of cell components reveals the dynamics of subcellular re-organization in response to infection of Arabidopsis by oomycete pathogens. *Plant J.* **33**, 775–792.
- Takemoto, D., Jones, D.A. and Hardham, A.R. (2006) Re-organization of the cytoskeleton and endoplasmic reticulum in the Arabidopsis *pen1-1* mutant inoculated with the non-adapted powdery mildew pathogen, *Blumeria graminis* f. sp. *hordei*. *Mol. Plant Pathol.* **7**, 553–563.
- Thieme, F., Szczesny, R., Urban, A., Kirchner, O., Hause, G. and Bonas, U. (2007) New type III effectors from *Xanthomonas campestris* pv. *vesicatoria* trigger plant reactions dependent on a conserved N-myristoylation motif. *Mol. Plant Microbe Interact.* **20**, 1250–1261.
- Tyler, B.M., Tripathy, S., Zhang, X. et al. (2006) *Phytophthora* genome sequences uncover evolutionary origins and mechanisms of pathogenesis. *Science*, **313**, 1261–1266.
- Tytgat, T., Vercauteren, I., Vanholme, B., De Meutter, J., Vanhoutte, I., Gheysen, G., Borgonie, G., Coomans, A. and Gheysen, G. (2005) An SXP/RAL-2 protein produced by the subventral pharyngeal glands in the plant parasitic root-knot nematode *Meloidogyne incognita*. *Parasitol. Res.* **95**, 50–54.
- Valent, B. and Khang, C.H. (2010) Recent advances in rice blast effector research. *Curr. Opin. Plant Biol.* **13**, 434–441.
- Voegelé, R.T. and Mendgen, K. (2011) Nutrient uptake in rust fungi: how sweet is parasitic life? *Euphytica*, **179**, 41–55.
- Wang, W., Devoto, A., Turner, J.G. and Xiao, S. (2007) Expression of the membrane-associated resistance protein RPW8 enhances basal defense against biotrophic pathogens. *Mol. Plant Microbe Interact.* **20**, 966–976.
- Wang, W., Wen, Y., Berkey, R. and Xiao, S. (2009) Specific targeting of the Arabidopsis resistance protein RPW8.2 to the interfacial membrane encasing the fungal haustorium renders broad-spectrum resistance to powdery mildew. *Plant Cell*, **21**, 2898–2913.
- Whisson, S.C., Boevink, P.C., Moleleki, L. et al. (2007) A translocation signal for delivery of oomycete effector proteins into host plant cells. *Nature*, **450**, 115–118.
- Win, J., Morgan, W., Bos, J., Krasileva, K.V., Cano, L.M., Chaparro-Garcia, A., Ammar, R., Staskawicz, B.J. and Kamoun, S. (2007) Adaptive evolution has targeted the C-terminal domain of the RXLR effectors of plant pathogenic oomycetes. *Plant Cell*, **19**, 2349–2369.
- Wu, S., Lu, D., Kabbage, M., Wei, H.L., Swingle, B., Records, A.R., Dickman, M., He, P. and Shan, L. (2011) Bacterial effector HopF2 suppresses Arabidopsis innate immunity at the plasma membrane. *Mol. Plant Microbe Interact.* **24**, 585–593.